Correcting Spatial Distortion and non-Uniformity in Planar Images from γ-Camera Systems

D. Thanasas, D. Maintas, E. Georgiou, N. Giokaris, A. Karabarbounis, C.N. Papanicolas and E. Stiliaris

***Abstract*–In this work a correction method for the spatial distortion and non-uniformity of planar images is presented. It is based on an event-by-event correction algorithm suitable for images obtained from small Field of View (FOV) γ-Camera systems which are equipped with a Position Sensitive PhotoMultiplier Tube (PSPMT). In our study, the γ-Camera system consists of a 3 inch PSPMT with a 16X+16Y crossed wire anode (Model R2486, HAMAMATSU), a 4mm pixelated CsI(Tl) crystal (pixel-width 1mm) and a parallel (hexagonal) hole collimator. The correction of the spatial distortion is based on lookup tables with the coordinates of well defined reference points which are selected during the calibration phase of the system. The reference points are the centres of predefined pixels, well distinguishable at the planar image using a small laboratory ^{60}Co source without collimation. The applied algorithm incorporates 2D-interpolation techniques and has been developed on a full automated graphics environment making use of the HIGZ (High Level Interface to Graphics and Zebra) program libraries from CERN. Both correction methods for the spatial distortion and non-uniformity have been applied to planar images obtained from small capillary phantoms filled with water solution of ^{99m}Tc. The method is also extended to tomographic images and the observed SPECT improvement in resolution is discussed.**

I. Introduction

In nuclear medicine a number of small field, high-resolution γ-Camera systems based on PSPMT have been recently developed [1]-[4]. Their advantages over commercial γ-Camera systems (better spatial resolution, lower cost, light weight) justify their demand for imaging of small human body organs or small animals. However, the existence of spatial distortions and non-uniformities are very common problems in images from small field γ-Camera systems [5]-[7]. These problems result in a weakening of the quality and the clinical value of the image. It is thus very important to develop correction methods in order to overcome these distortions. For this reason, several methods for correcting this kind of nonlinearities have been investigated [8],[9].

This work is partially supported by the 03EΔ287 research project, implemented within the framework of the "Reinforcement Programme of Human Research Manpower" (PENED) and co-financed by National and Community Funds (25% from the Greek Ministry of Development-General Secretariat of Research and Technology and 75% from E.U.-European Social Fund). The financial support by the program KAPODISTRIAS (Special Account for Research Grants) of the National and Kapodistrian University of Athens is gratefully acknowledged.

D. Thanasas, N. Giokaris, A. Karabarbounis, C.N. Papanicolas and E. Stiliaris are with the National and Kapodistrian University of Athens, Department of Physics, 15771 Athens, Greece.

D. Maintas is with the Institute of Isotopic Studies, Athens, Greece.

E. Georgiou is with the National and Kapodistrian University of Athens, Medical School, Athens, Greece.

Corresponding author: E. Stiliaris (e-mail: stiliaris@phys.uoa.gr)

The novel method presented here corrects offline, event by event, the spatial distortions of planar images. It makes use of a correction table, whose elements are derived from a calibration planar image after irradiation of the crystal in use with a ^{60}Co point source. Based on this technique, the nominal coordinates of all detected data points can be calculated and consequently the spatial distortions and non-uniformities of raw images can be repaired. In the following, the correction method is applied to experimental results from phantom planar images and it is extended to SPECT data. Both corrected and uncorrected results are shown for comparison and the obtained improvement in the spatial resolution and uniformity is discussed.

II. The γ - Camera System

The main components of the γ-Camera system are a PSPMT (model HAMAMATSU R2486) [10], a 4mm thick pixelated CsI(Tl) scintillation crystal with 1mm pixel-width and finally a 27mm thick parallel-hole, lead collimator. The 3-inch in diameter cylindrical PSPMT is composed of a Bialkali photocathode, a 12-stage coarse mesh dynode structure and 16X+16Y crossed-wired anodes arranged into two orthogonal groups. The anode output wires are connected to a resistive current divider network so that the number of the readout analogue signals is reduced to four $\{X_A, X_B, Y_C, Y_D\}$. Both the energy (E) and the position (X,Y) of the incident γ-rays can be reconstructed from these four signals through the following equations:

$$X = \frac{X_A - X_B}{X_A + X_B},\ Y = \frac{Y_C - Y_D}{Y_C + Y_D}$$

$$E = X_A + X_B + Y_C + Y_D$$

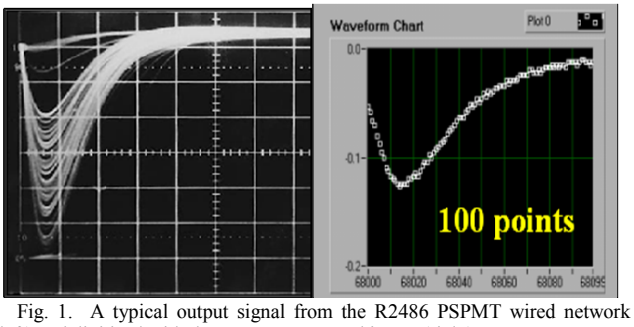

Fig. 1. A typical output signal from the R2486 PSPMT wired network (left) and digitized with the 20 MHz-PCI card in use (right).

The readout system [11] comprises a fast Analogue to Digital Converter (ADC) on a PCI card (model PCI-9812 ADLink) [12], with four single-ended input channels that lead to four A/D converters simultaneously running with a maximum sampling rate of 20 MHz. A typical digitization of an analogue input signal is shown in Fig. 1. The whole digitizing and data acquisition system (DAQ) is controlled by software developed on the LabVIEW environment (Fig. 2).

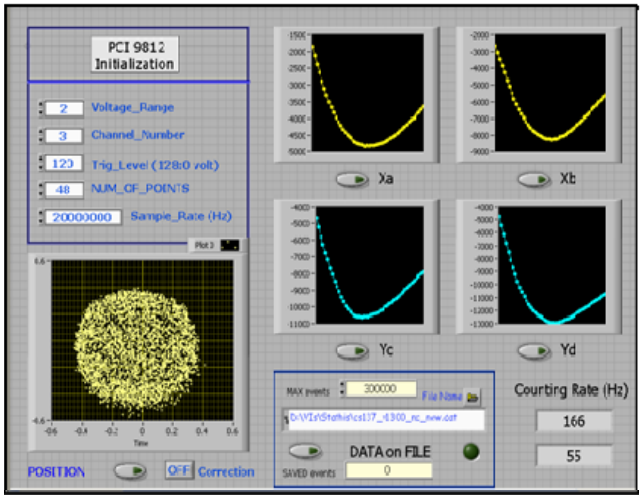

Fig. 2. Interface of the data acquisition program developed on the LabVIEW environment .

III. The Correction Algorithm

The calibration planar image acquired after irradiation of the pixelated crystal with a ^{60}Co point source, without using the collimator, placed at a distance of about 5 times the FOV far from the crystal surface is shown in the top of Fig. 3. Offline cut-offs of the low energetic photons have been applied in this case. Although the squared 1mm×1mm pixels of the crystal are clearly visible in this planar projection, the quality of the image is weakened by a characteristic spatial distortion, known as barrelloid distortion, which mostly appears at the peripheral region of γ-Camera's FOV.

The method used to overcome this distortion problem is mainly based on a 2-dimensional interpolation technique using both, a correction- and a reference-table. The correction table includes the coordinates (X_t,Y_t) of a number of selected pixels (Fig. 4, left) mostly from the outer region of the FOV, where the distortion is greater. The elements of this table are extracted from the calibration planar image and automatically stored is a correction file with the help of a graphical interface. This application has been developed in FORTRAN and linked to the HIGZ (High level Interface of Graphics and ZEBRA) package from CERN. In addition, the nominal coordinates (X'_t,Y'_t) of the selected pixels, which are well known through the geometry and the orientation of the pixelated crystal in use (Fig. 4, right), are stored in a reference table and a corresponding file with all these reference values is also created.

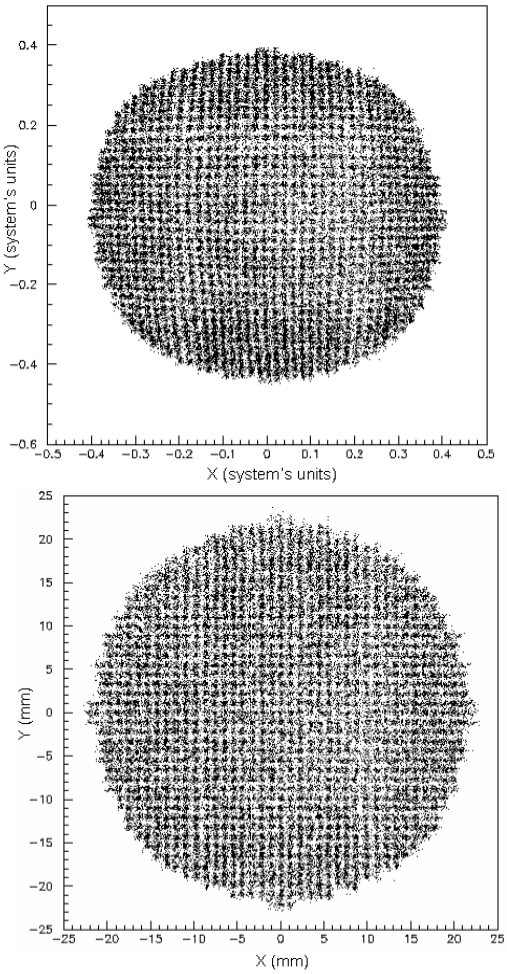

Fig. 3. Uncorrected (top) and corrected (bottom) planar images of the pixelated crystal CsI(Tl) after irradiation with a ^{60}Co point source without the use of any collimation. A software cut-off on the low energetic photons has been applied in this case. Distances are measured in system's units in the uncorrected image and in mm in the corrected image.

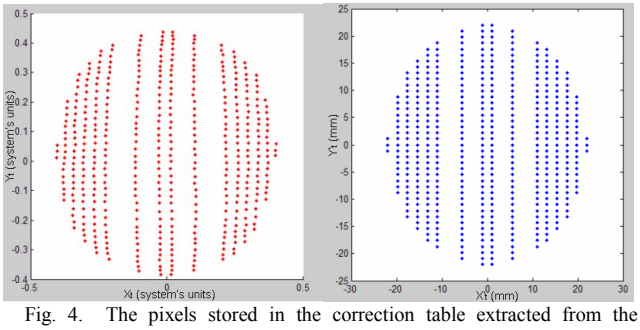

Fig. 4. The pixels stored in the correction table extracted from the calibration planar image (left) and their nominal values (right) stored in the reference table.

The formalism used to correct the position of any detected point (X,Y) is briefly described in the following. Firstly, the two aspect ratios *a* and *b* for the detected point are calculated according to the equations:

$$a = \frac{X - X_{t,i}}{X_{t,i+1} - X_{t,i-1}},\ b = \frac{Y - Y_{t,j}}{Y_{t,j+1} - Y_{t,j-1}}$$

where, $(X_{t,i},Y_{t,j})$ are the coordinates of the nearest to the detected point element of the correction table. Consequently, it's corrected position (X_{cor},Y_{cor}) is

$$X_{cor} = X'_{t,i} + a \cdot (X'_{t,i+1} - X'_{t,i-1})$$

$$Y_{cor} = Y'_{t,j} + b \cdot (Y'_{t,j+1} - Y'_{t,j-1})$$

with $(X'_{t,i},Y'_{t,j})$ being the nominal values of $(X_{t,i},Y_{t,j})$, as they are stored in the reference table. The above technique is schematically described in Fig. 5. The algorithm applies on an event-by-event basis and can be used offline to extend a measured data-file to contain in addition the information of the corrected position.

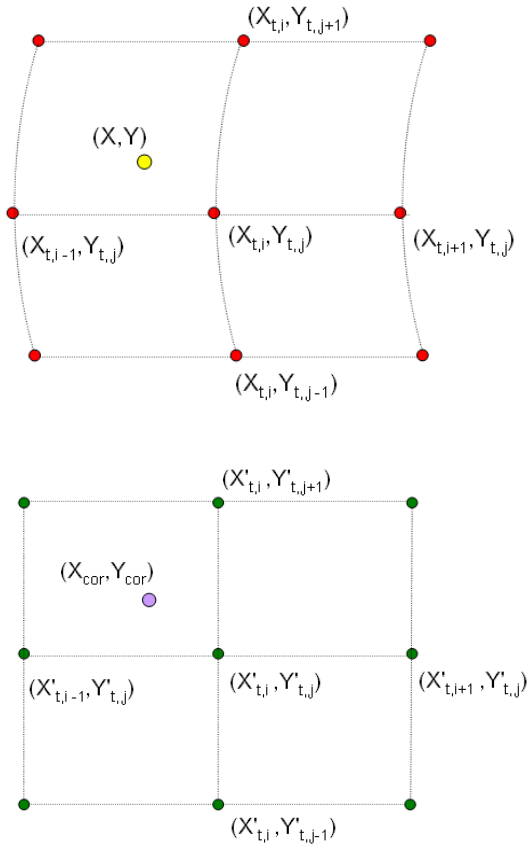

Fig. 5. Schematic description of the spatial correction algorithm. The coordinates of a detected data point (top) are corrected (bottom) by applying 2D-interpolation techniques based on predefined selected pixels.

Moreover, non-uniformity of the photon intensity is observed in planar images (as shown in Fig. 6) which can be calculated and corrected. Uniformity is partially improved with the previously described algorithm of the spatial correction. This is reflected in the ratio I_{min}/I_{max} of the global detected photon intensity minimum (I_{min}) to the global detected maximum (I_{max}) for a uniformly irradiated area. This ratio changes from 0.33 in the case of a position-uncorrected image to 0.44 after the application of spatial correction method. A special technique is further developed to bring this ratio to the ideal value of I_{min}/I_{max}=1.00. With an appropriate binning scheme, multiplication factors, inversely proportional to the measured photon intensity, are stored in a reference density matrix. This matrix can be later applied to any reconstructed planar image to balance the intensity caused by the inhomogeneous efficiency of the system.

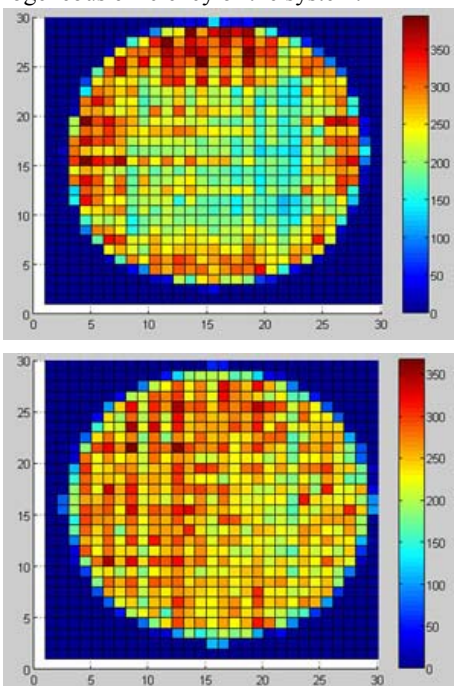

Fig. 6. Photon intensity measurements of the uncorrected (top) and corrected (bottom) planar images of Fig. 3 using 30x30 binning scheme.

IV. SPECT IMAGING

The effect of the previously described corrections to the SPECT imaging has also been studied. Data were collected with the full functioning γ-Camera system for a rotating phantom shown in Fig. 7. The phantom consists of four thin capillaries (1.2mm outer diameter) filled with ^{99m}Tc. They are placed in 10mm distance parallel to each other and form an orthogonal squared prism. Twelve planar images were acquired in steps of 15^{o} by applying the previously described spatial and uniformity correction. Tomographic images were reconstructed using custom made algorithms based on the Maximum-Likelihood Expectation Maximization (MLEM) method.

Corrected and uncorrected tomographic images for different heights, 15mm and 0mm from the center of the FOV, are presented in Fig. 8. As expected, spatial distortion and non-uniformity are more dominant at the periphery than at the central region of the FOV. No differences are observed between the corrected and uncorrected planar images for cuts near the center.

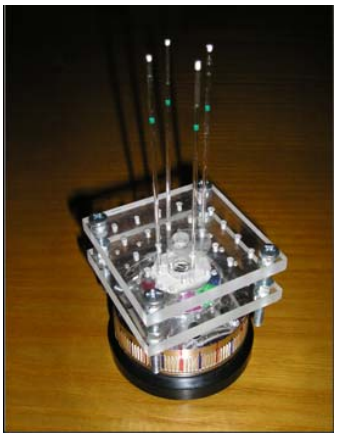

Fig. 7. Rotating phantom of four capillaries filled with ^{99m}Tc solution, forming an orthogonal prism.

Finally 3D reconstructed images, corrected and uncorrected, of the same phantom are depicted in Fig. 10. Due to barrel-distortion, at the uncorrected level the capillaries appear to be curved, while the applied corrections improve adequately the image quality.

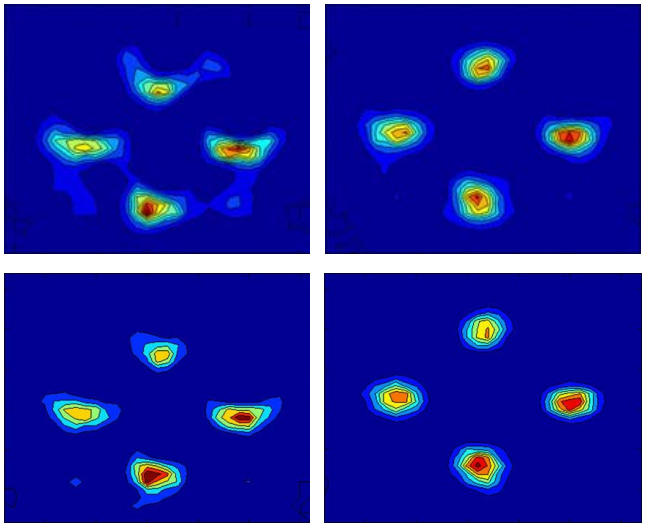

Fig. 8. Reconstructed tomographic images of four capillaries at the height of 15mm (top) and 0mm (bottom) from the center of the FOV using uncorrected (left) and corrected (right) projection data.

V. Concluding Remarks

The developed correction methods for spatial distortion and non-uniformity which appear in planar images of small FOV γ-Camera systems, using pixelated crystals, have been successfully applied to planar and tomographic level and show indisputably the overall improvement of the image quality. Comparative images studied so far show that the position correction method improves also their uniformity. The method will also be extended in the future to images acquired from homogeneous crystals using the collimator in order to create the correction and reference tables. Further investigations and quantification of the image (raw and corrected) resolution are under way. Future use of these techniques on a clinical level is also planned.

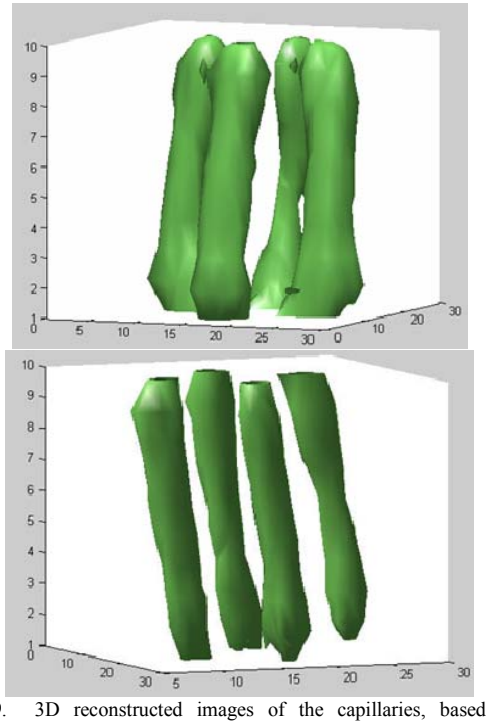

Fig. 9. 3D reconstructed images of the capillaries, based on the uncorrected (top) and corrected (bottom) planar images with distances measured in mm.

References

[1] G. K. Loudos *et al.*, "A 3D high-resolution gamma camera for radiopharmaceutical studies with small animals", *Applied Radiation and Isotopes*, vol. 58, pp. 501-508, 2003.

[2] R. Pani *et al.*, "A novel compact gamma camera based on flat panel PMT", *Nucl. Instrum. and Methods A*, vol. 513, pp. 36-41, 2003.

[3] F. Sanchez *et al.*, "Performance tests of two portable mini gamma cameras for medical applications", *Med. Phys.*, vol. 33, pp. 4210-4220, 2006.

[4] C. Trotta, R. Massari, N. Palermo, F. Scopinaro, A. Soluri, "New high spatial resolution portable camera in medical imaging", *Nucl. Instrum. and Methods A*, vol. 577, pp. 604-610, 2007.

[5] R. Pani *et al.*, "A compact gamma ray imager for oncology", *Nucl. Instrum. and Methods A*, vol. 477, pp. 509-513, 2002.

[6] M. M. Fernandez *et al.*, "A flat-panel-based mini gamma camera for lymph nodes studies", *Nucl. Instrum. and Methods A*, vol. 527, pp. 92-96, 2004.

[7] Myung Hwan Jeong *et al.*, "Performance improvement of small gamma camera using NaI(Tl) plate and position sensitivephoto-multiplier tubes", *Phys. Med. Biol.*, vol. 49, pp. 4961–4970, 2004.

[8] I. Buvat, H. Benali, A. Todd-Pokropek and R. DiPaola, "A new correction method for gamma camera nonuniformity due to energy response variability", *Phys. Med. Biol.*, vol. 40, pp. 1357–1374, 1995.

[9] Timothy K. Johnson, Charles Nelson and Dennis L. Kirch, "A new method for the correction of gamma camera nonuniformity due to spatial distortion", *Phys. Med. Biol.*, vol. 41, pp. 2179–2188, 1996.

[10] Hamamatsu Technical Data Sheet, "Position Sensitive Photomultiplier Tubes With Crossed Wired Anodes R2486 Series", Hamamatsu Photonics, 1998.

[11] V. Spanoudaki *et al.*, "Design and development of a position-sensitive γ-Camera for SPECT imaging based on PCI electronics", *Nucl. Instrum. and Methods A*, vol. 527, pp. 151-156, 2004.

[12] ADLink Data Sheet, "PCI 9812/9810 20 MHz Simultaneous 4-CH Analog Input Cards", ADLink Technology, 2003.